Cu (II) and ammonium adsorption from dairy cattle breeding sewage by phosphorus-modified dairy cow manure hydrochar

Zhendong Yang[1], Min Tong[2], Xueqin He[1], Lujia Han[1], Jianbin Guo[1], Tianjun Jing[3], Guangqun Huang[1*], Changming Shi[2*]

(1. *College of Engineering*, *China Agricultural University*, *Beijing 100083*, *China*;
2. *Electric Power Research Institute of State Grid East Inner Mongolia Electric Power Co., Ltd, Hohhot 010010, Inner Mongolia, China*;
3. *College of Information and Electrical Engineering*, *China Agricultural University*, *Beijing 100083*, *China*)

Abstract: To realize the synergistic treatment of dairy cow manure solids and dairy cattle breeding sewage, this study produced phosphorus-modified hydrochar by dairy cow manure solids impregnated with potassium phosphate (K_3PO_4). And then, the adsorption characteristics of Cu (II) and ammonium (NH_4^+) in dairy cattle breeding sewage under different dosages and adsorption time conditions of modified hydrochar were explored. The results show that the specific surface area and total pore volume of the hydrochar were increased by phosphorus-modified. The adsorption amount of hydrochar per unit-mass decreased with the increase in the dosage. With the increase in the dosage, the adsorption capacity of Cu (II) decreased from the initial 26.16 mg/g to 3.38 mg/g. The adsorption of Cu (II) and NH_4^+ in sewage by hydrochar was mainly chemical adsorption, which was mainly affected by chelation and ion exchange. This adsorption was more inclined to single-molecular layer adsorption. Both the pH values and the ionic strength influenced the competitive adsorption between Cu (II) and NH_4^+. The higher the pH value was, the greater the adsorption amount, and the stronger the adsorption capacity by hydrochar. Moreover, the increase in the ionic strength decreases the adsorption capacity of hydrochar.

Keywords: dairy manure, hydrochar, sewage, adsorption, competitive adsorption
DOI: 10.25165/j.ijabe.20221505.7640

Citation: Yang Z D, Tong M, He X Q, Han L J, Guo J B, Jing T J, et al. Cu (II) and ammonium adsorption from dairy cattle breeding sewage by phosphorus-modified dairy cow manure hydrochar. Int J Agric & Biol Eng, 2022; 15(5): 78–84.

1 Introduction

The intensive development of dairy farming in China has produced a large amount of manure, which has the characteristics of high solids, high oxygen consumption, and high ammonia nitrogen. Untreated exposure of this manure to the air will release malodorous gases and greenhouse gases[1]. In addition, dairy cow manure contains a large amount of unstable organic matter and a high ratio of carbon to nitrogen (C/N)[2]. The heavy metal content of dairy cow manure is also high, which could cause severe deterioration of surface water or groundwater quality, resulting in serious environmental pollution problems. In order to avoid the above problems and realize resource utilization of dairy cow manure, solid-liquid separation pretreatment is usually used, and then the solids and sewage of the dairy cow manure are treated cooperatively[3].

Liquid-phase sewage was treated mainly by chemical precipitation and adsorption[4]. Recently, biotechnology, photocatalysis, and genetic engineering were also been used and studied in manure treatment[5]. The adsorption method was commonly used and prevalent because of its simple operation and good treatment effect. Activated carbon has an efficient absorption of abundant waste, such as heavy metal, ions, and organic waste, but it is hard to reuse and regenerate. Although the regeneration process of adsorption resin is more straightforward than activated carbon, its price is higher. Therefore, it is of great practical significance to develop adsorbent materials with low cost and good adsorption performance due to industrial demand orientation.

In recent years, researchers have used different biomass materials to obtain different types of hydrothermal products through specific carbonization conditions, and then using them to treat sewage has become a hot spot. Liu[6] developed a hydrochar by using sludge and coconut shells and found that the adsorption process belongs to monolayer adsorption, accompanied by a spontaneous endothermic process. Mirva et al.[7] found that the oxygen-containing functional groups on the surface played an essential role in the adsorption of methylene blue when studying the adsorption properties of horse manure hydrochar. Kaewtrakulchai et al.[8] found that by modifying horse manure hydrochar, its adsorption performance can be greatly improved, and the prepared biochar has the advantages of environmental friendliness, low cost, and easy availability of raw materials. It is pointed out that the adsorption properties of hydrochar can be effectively improved by modifying[9]. Existing studies have

Received date: 2022-04-28 **Accepted date:** 2022-08-17
Biographies: Zhendong Yang, MS, research interest: agricultural biomass resource utilization, Email: yangzhendong@cau.edu.cn; **Min Tong**, MS, Engineer, research interest: biomass resource comprehensive utilization, Email: 346980594@qq.com; **Xueqin He**, PhD, research interest: agricultural equipment/biomass engineering, Email: hxq12@cau.edu.cn; **Lujia Han**, PhD, Professor, PhD, Professor, research interest: agricultural biomass engineering, Email: hanlj@cau.edu.cn; **Jianbin Guo**, PhD, research interest: agricultural biomass utilization, Email: jianbinguo@cau.edu.cn; **Tianjun Jing**, PhD, research interest: New energy power generation control, Email: jtjy11@cau.edu.cn.
***Corresponding author: Guangqun Huang**, PhD, Professor, research interest: agricultural equipment/biomass engineering. College of Engineering, China Agricultural University, Beijing 100083, China. Tel: +86-10-62737995, Email: huanggq@cau.edu.cn; **Changming Shi**, Bachelor, Senior Engineer, research interest: biomass engineering. Electric Power Research Institute of State Grid East Inner Mongolia Electric Power Co., Ltd, Hohhot, 010010, Inner Mongolia, China. Tel: +86-471-6215878, Email: 66158692@qq.com.

shown that phosphorus-containing materials can effectively adsorb and fix harmful substances such as heavy metals, and phosphate radicals play an essential role[9]. As a common phosphate, potassium phosphate (K_3PO_4) is easy to obtain. However, there are few reports on the use of phosphate to modify the hydrochar and explore its adsorption of pollutants in aquaculture sewage to improve the phosphorus content of the hydrochar.

In summary, the modified biomass-based hydrochar can be used for various sewage treatments and its adsorption effect is ideal. However, the current research primarily uses simulated sewage, which is different from the actual sewage composition and cannot meet the current industrial urgent needs. In this study, the solids and sewage after solid-liquid separation of dairy cow manure were taken as the objects. They were investigated by preparing modified biochar, and the effects of dosage and adsorption time on the adsorption of Cu (II) and ammonium (NH_4^+) in sewage were studied. The adsorption model was fitted, and the competitive adsorption characteristics of Cu (II) and NH_4^+ were explored to provide methodological and data support for industrial applications.

2 Materials and methods

2.1 Experimental materials

The cow manure for producing hydrochar was collected after solid-liquid separation from the Jinyindao Ranch, Daxing District, Beijing. The Treasure Island Ranch is affiliated with Shounong Animal Husbandry. It is a modern large-scale dairy farm and a local representative dairy farming base. The number of dairy cows is large, and the demand for manure treatment is also large, so this dairy farm is selected as a pilot for sample collection and factory testing. The samples were stored in a freezer at −20°C. A 100 g manure sample was dried at 105°C for 24 h to determine its moisture content. The dried samples were smashed through a 0.5 mm sieve with a cyclone mill (ZM200, Leitch, Germany), and stored in a sealed bag.

Dairy cattle breeding sewage was taken from the liquid part of cow manure after solid-liquid separation in Jinyindao Ranch, Daxing District, Beijing. Since it still contains some solids, the liquid part of cow manure after solid-liquid separation was left to settle and filter before the absorption test.

2.2 Experimental methods

2.2.1 Preparation of modified hydrochar

Hydrochar was prepared by a hydrothermal carbonization reactor which was a high-temperature and high-pressure reactor (Parr 4523, USA). An amount of cow manure sample (converted to dry basis weight is 30 g) with adding 3 g K_3PO_4 was thoroughly mixed to make the final solid-liquid ratio reach 1:12 by adding proper deionized water[10]. The N_2 gas was passed through for 10 min, and the air in the reactor was discharged by circulating and venting to keep it in an inert gas atmosphere. The reaction temperature was set to 260°C and the holding time was 6 h. After the reaction was completed, the set temperature was lowered to 20°C, and the valve was opened to flow cooling circulating water to cool the tank. After the reactor was lowered to room temperature, the material was taken out and filtered. The solid was dried at 105°C for 24 h, cooled to room temperature, and stored in a sealed bag[11].

2.2.2 Characterization of physicochemical properties of hydrochar

Scanning Electron Microscope (SEM) is often used to observe the surface features of objects, and Fourier Transform Infrared Spectroscopy (FT-IR) is often used to characterize the surface functional group structure of materials, which can be used to determine different molecular bonds (such as a single bond, double bond). Element Analyzer can be used to determine the content of C, H, N, S, and other elements in the sample. The modified hydrochar-specific surface area and pore size distribution were measured using a Surface Area Analyzer.

2.2.3 Basic adsorption

1) Different dosages of hydrochar

Weigh 0.01, 0.03, 0.05, 0.08, 0.10, and 0.20 g of hydrochar and 200 mL of sewage, respectively, and add them to 250 mL beakers for adsorption experiments. After reaching the predetermined time (6 h), the Cu (II) and NH_4^+ concentrations were measured[12-14].

2) Different adsorption time

Weigh 0.05g of hydrochar and 200 mL of sewage into a 250 mL beaker for adsorption test. The water bath is kept at a constant temperature of 25°C and stirred at a speed of 200 r/min. The set times are 15 min, 30 min, 1 h, 2 h, 4 h, 6 h, 8 h, and 10 h respectively. The process conditions for membrane filtration and determination of Cu (II) and NH_4^+ concentrations after reaching the predetermined time are the same as above.

2.2.4 Cu (II) and NH_4^+ competitive adsorption experiments

There are many factors that affect competitive adsorption, such as temperature, pH, ionic strength, cation exchange capacity, redox potential, and so on. This paper mainly selects pH and ionic strength which are easy to control in factory applications for studying.

Using the batch equilibrium adsorption method, weigh 0.1g of hydrochar and place it in a 50 mL round-bottomed plastic centrifuge tube with a stopper. Use $NaNO_3$ solution (concentrations of 0.002, 0.01, and 0.05 mol/L, respectively) as the background solution to prepare the concentration. Configure the gradient solution with 50, 100, 200, 300, 400, and 500 mg/L of Cu (II) and 40, 80, 160, 240, 320, and 400 mg/L of NH_4^+, and adjust the initial pH of the solution to 4.5, 5.0, 5.5. According to the solid-liquid ratio of 1:10, add mixed solutions of different concentrations into the centrifuge tube, plug, and seal. Shake with a constant temperature oscillator for 24 h under the constant temperature of 25°C. After filtration, the supernatant was taken to measure the concentrations of Cu (II) and NH_4^+[15]. The concentration of Cu (II) was measured by UV spectrophotometer, and the concentration of NH_4^+ was measured by Kjeldahl nitrogen analyzer, with three repetitions.

2.2.5 Data and statistical analysis

The pseudo-first-order kinetic equation is a chemical kinetic equation based on the regulatory relationship between reactant concentrations and reaction rates. The pseudo-first-order kinetic model can reflect the linear relationship between reaction rate and reactant concentration. The pseudo-second-order kinetic model assumes that the adsorption rate is governed by a chemisorption mechanism involving electron sharing or electron transfer between the adsorbent and the adsorbate. The pseudo-first-order kinetic equation is[16]

$$\frac{dq_t}{dt} = k_1(q_e - q_t) \tag{1}$$

where, q_e is the adsorption capacity of the adsorbent to the adsorbate per unit mass at the adsorption equilibrium, mg/g; q_t is the adsorption capacity of the adsorbent to the adsorbate at time t, mg/g; k_1 is the same as first order kinetic model adsorption rate constant, min^{-1}.

The pseudo-second-order kinetic equation is[17]

$$\frac{dq_t}{dt} = k_2(q_e - q_t)^2 \quad (2)$$

where, k_2 is subject to second order kinetic model adsorption rate constant, min^{-1}.

Langmuir's adsorption isotherm equation and the Freundlich adsorption isotherm equation were used to fit the adsorption isotherm data. The Langmuir model assumed that the adsorption was monolayer, with no other molecular covering, and that the probability of the adsorbate occupying all adsorption sites was the same. At the same time, the surface of the adsorbent was entirely uniform, and the probability of a molecule being adsorbed on a site was independent of whether other molecules already occupied the adjacent space. The Freundlich adsorption isotherm model is a semi-empirical model describing heterogeneous adsorption systems. If the solid surface of the adsorbent is not uniform, the adsorption equilibrium constant will be related to the surface coverage.

The linear form of the Langmuir adsorption isotherm equation is as follows[18]:

$$\frac{C_e}{q_e} = \frac{1}{q_0 b} + \frac{C_e}{q_0} \quad (3)$$

where, C_e is the equilibrium concentration, mg/L; q_0 is the saturated adsorption capacity of the adsorbent, mg/g; b is the Langmuir adsorption constant, L/mg.

The Freundlich isotherm adsorption equation is expressed as follows[19]:

$$q_e = KC_e^{1/n} \quad (4)$$

where, K is the Freundlich adsorption equilibrium constant, reflecting the strength of the adsorption capacity; $1/n$ is the component factor, indicating the adsorption capacity increases with the concentration, reflecting the difficulty of adsorption.

Adsorption kinetics were simulated by Matlab 2021 (MathWorks Co. Ltd, USA). Figures were performed using OriginPro 2022 (OriginLab Co.td, USA).

3 Results and discussion

3.1 Characterization of hydrochar

3.1.1 SEM analysis

Figure 1 shows the SEM images of the hydrochar before and after modification. Under the same reaction temperature and holding time, the surface morphology of the hydrochar did not change much, and the resulting carbon microspheres had good sphericity but poor dispersibility and poor uniformity. However, after being modified by K_3PO_4, the structure of hydrochar became sparser, and the density of microspheres was lower. Because the fibrous structure of cow manure was destroyed, the soluble carbohydrates were dissolved from the carbon skeleton, and more fragmented structures appeared. However, the original carbon skeleton was stable, to the final product structurally was similar to the unmodified one[19].

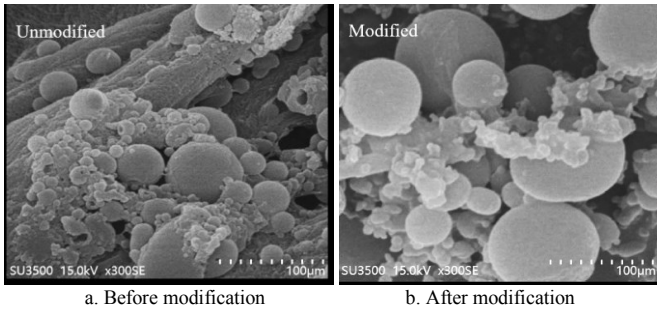

a. Before modification b. After modification

Figure 1 SEM images of hydrochar before and after modification

3.1.2 FT-IR analysis

In Figure 2, the K_3PO_4 modified cow manure hydrochar contained more large surface functional groups than the unmodified one, which was more conducive to its adsorption of pollutants in sewage. 3400 cm^{-1} was the stretching vibration peak of the N-H bond, and 1653 cm^{-1} was the bending vibration peak of the N-H bond, both of which had improved intensities after modification. 1530 cm^{-1} was the bending vibration peak of C=O, indicating that K_3PO_4 modification could reduce the fatty group, ketone group, and ester substances of cow manure. In addition, the peak generated at 2925 cm^{-1} was the C-H symmetrical stretching vibration of CH, CH_2, CH_3, and other groups in the aliphatic hydrocarbon mechanism, and the peak intensity in the K_3PO_4 modified cow manure sample was reduced.

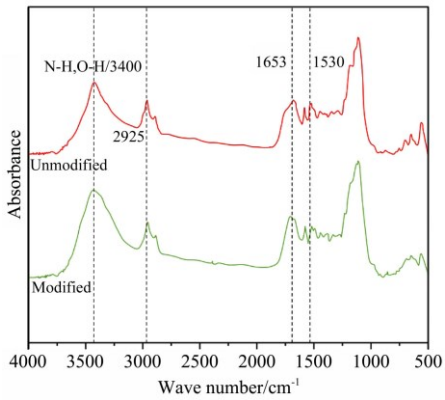

Note: FT-IR: Fourier Transform Infrared Spectroscopy. The black dotted line reflects a certain wave number, such as 2925 cm^{-1}, 1653 cm^{-1}, 1530 cm^{-1}, and 3400 cm^{-1}.

Figure 2 FT-IR spectra of hydrochar before and after modification

3.1.3 Elemental composition, industrial composition, and surface area analysis

The elements and industrial compositions of cow manure hydrochar before and after modification are shown in Table 1. The carbon content of the K_3PO_4 modified cow manure hydrochar increased, indicating that the K_3PO_4 modifier promoted the hydrothermal reaction. The atomic ratios of H/C and O/C decreased, indicating that the aromaticity and hydrophobicity of the modified hydrochar were enhanced, and some non-polar functional groups were formed on the surface of the hydrochar during the modification process. The ash content of the modified hydrochar was also higher than that before the modification, indicating that the K_3PO_4 treatment promoted the formation of new inorganic functional groups on the surface of the hydrochar, which was beneficial to the adsorption of pollutants. The ash content of the hydrochar samples increased after adsorption, indicating that the hydrochar adsorbed more inorganic substances. The modified hydrochar specific surface area and total pore volume increased by 1.65% and 1.32%, respectively. The reason might be that K_3PO_4 had a particular catalytic effect on the hydrothermal process, which destroyed the fiber structure of cow manure. Moreover, the phosphoric acid generated by the decomposition of K_3PO_4 was beneficial to the opening of some tiny pores of the cow manure, thereby increasing the specific surface area; the pore size distribution of the modified hydrochar was relatively wide in the range of 1.32-22.98 nm, which was typical porous and microporous adsorbents.

3.2 Adsorption characteristics of hydrochar

3.2.1 Effects of hydrochar dosage and adsorption time

Figure 3 shows the effects of hydrochar dosage and adsorption

time on the adsorption properties of Cu (II) (q_1) and NH_4^+ (q_2) at 25°C.

Table 1 Elemental composition, industrial composition, and surface area analysis of hydrochar

Sample		Unmodified	Modified
Elemental analysis	C/%	44.37±4.28	46.33±5.25
	H/%	4.58±0.77	4.62±0.38
	N/%	2.23±0.26	2.76±0.18
	S/%	0.57±0.04	0.56±0.06
	O/%	23.25±4.21	17.35±3.24
Industrial analysis	VM/%	55.42±5.33	49.25±6.84
	FC/%	19.48±1.94	23.99±2.81
	Ash/%	25.12±7.23	26.76±9.22
Specific surface area/$m^{-2}\cdot g$		21.56	25.78
Average pore size/nm		4.34	4.25
Total pore volume/$cm^{-3}\cdot g$		0.0318	0.0322

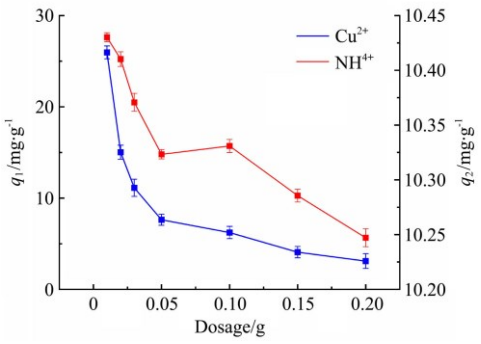

a. Hydrochar dosage

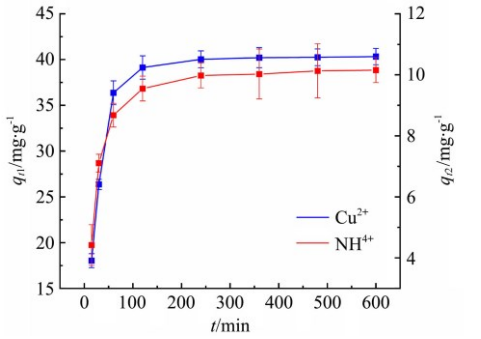

b. Adsorption time

Note: q_1 represents the adsorption properties of Cu (II); q_2 represents the adsorption properties of NH_4^+.

Figure 3 Effects of hydrochar dosage and adsorption time on the adsorption properties of Cu (II) and NH_4^+ at 25°C

The adsorbent dosage was an essential factor affecting the adsorption process, which determines the adsorbent-adsorbate equilibrium of the system[17]. In Figure 3, with the increase in dosage, the adsorption capacity of hydrochar to Cu (II) and NH_4^+ decreased. The reason was that the increase in hydrochar dosage made the adsorption sites increase, so the total adsorption capacity increased. However, when the dosage increased, the surface of the hydrochar was prone to agglomeration, which caused the pore channels on the surface to block each other, and not all adsorption active sites were effectively utilized. At the same time, with the progress of adsorption, the concentrations of Cu (II) and NH_4^+ in the solution decreased so that they could not enter the adsorption active sites of the hydrochar rapidly and in large quantities[18]. Therefore, the adsorption capacity of hydrochar per unit mass decreased gradually with the increase in dosage. For Cu (II), due to the low concentration of Cu (II) in the sewage, the dosage has a great influence on the adsorption capacity of the hydrochar. With the increase in the dosage, it decreased from the initial 26.16 mg/g to 3.38 mg/g. However, due to the high content of NH_4^+ in sewage, the adsorption capacity of hydrochar decreased in the range of 0.01-0.20 g dosage, but the decrease was not significant, from the initial 10.43 mg/g to 10.24 mg/g. If it continues to increase the dosage, the adsorption capacity should be greatly reduced.

As shown in Figure 2 that the adsorption capacity of the hydrochar for Cu (II) and NH_4^+ increased very rapidly within the first 60 min. With the prolongation of adsorption time, the growth rate of the adsorption capacity of hydrochar for Cu (II) and NH_4^+ gradually slowed down, and the adsorption gradually approached saturation. After 240 min, the adsorption of Cu (II) and NH_4^+ by hydrochar reached equilibrium. With the extension of adsorption time to 480 min or even 600 min, the adsorption capacity of hydrochar remained stable. In the initial stage of adsorption, the concentrations of Cu (II) and NH_4^+ in the sewage were relatively high, and most of the adsorption sites on the surface of the hydrochar were not occupied, so the adsorption in the initial stage could proceed quickly. At this time, the adsorption is mainly concentrated on the surface of the hydrochar. With the prolongation of the adsorption time, the adsorption sites on the surface of the hydrochar were gradually occupied. After 240 min, as the concentrations of Cu (II) and NH_4^+ in the sewage gradually decreased, the active sites on the surface of the hydrochar were largely occupied and approached the saturation state. At the same time, there is mutual repulsion between the ions on the surface of the hydrochar. At this time, the Cu (II) and NH_4^+ plasmas need to overcome a large internal resistance if they want to enter the internal pores of the hydrochar. After 240 min, the adsorption rate became slower and slower, and finally reached equilibrium[13,14].

3.2.2 Adsorption kinetics

Table 2 lists the first-order kinetic fitting data of Cu (II) and NH_4^+ adsorption by hydrochar. The q_{e1} calculated by the first-order kinetic model fitting was 10.53 mg/g. In comparison, the $q_{e\,Cu}$ (q_e of Cu) measured was 42.59 mg/g, there was a large gap between them. The correlation coefficient R^2 obtained from the first-order kinetic model fitting was 0.66, indicating that the adsorption of Cu (II) by the hydrochar was not only physical adsorption but also affected by other adsorption methods[21].

Table 2 Fitting parameters of adsorption kinetic for Cu (II) and NH_4^+ adsorption by hydrochar

Kinetic model		Cu (II)	NH_4^+
Pseudo-first-order kinetics	q_e	42.59	10.42
	q_{e1}	10.53	7.35
	k_1	0.0037	0.0041
	R^2	0.66	0.74
Pseudo-second-order kinetics	q_e	42.59	10.42
	q_{e2}	41.32	10.44
	k_2	0.0020	0.0070
	h_0	3.5492	0.8420
	R^2	0.9992	0.9978

Note: q_e is the adsorption capacity of the adsorbent to the adsorbate per unit mass at the adsorption equilibrium, mg/g; q_{e1} is the saturated adsorption amount of Cu(II) by hydrothermal carbon calculated after fitting; k_1 is the same as order kinetic model adsorption rate constant, min^{-1}; q_{e2} is the saturated adsorption amount of NH_4^+ by hydrothermal carbon calculated after fitting; k_2 is subject to two order kinetic model adsorption rate constant, min^{-1}.

For the adsorption of NH_4^+, the q_{e2} calculated by the fitting was 2.33 mg/g, while the $q_{e\,N}$ (q_e of N) measured was 10.42 mg/g. The correlation coefficient R^2 was 0.74, indicating that the adsorption of

NH_4^+ by hydrochar had a poor fit with the first-order kinetic model, and the pseudo-first-order kinetic model was not suitable for describing the adsorption of NH_4^+ by hydrochar adsorption process.

The q_{e2} calculated by the second-order kinetic model for the adsorption of Cu (II) by the hydrochar was 41.84 mg/g, and the experimentally measured value $q_{e\ Cu}$ was 42.59 mg/g. Compared with the first-order kinetic model, the second-order kinetic model performed a more suitable simulation of the Cu (II) adsorption process by hydrochar. At the same time, the fitting coefficient of Cu (II) and the second-order kinetic model reached 0.9996, indicating that the adsorption model of Cu (II) by hydrochar should be closer to the second-order kinetic model, and the Cu (II) adsorption reaction process should belong to the chemical adsorption reaction process[22].

The second-order kinetic model was also more suitable for the adsorption process of NH_4^+ by hydrochar. The NH_4^+ adsorption capacity of the hydrochar was 10.44 mg/*g* calculated by the second-order kinetic model fitting, and the experimentally measured value q_{eN} = 10.42 mg/g. At the same time, the fitting coefficient between NH_4^+ and the second-order kinetic model reached 0.99971, indicating that the second-order kinetic model properly described the adsorption of NH_4^+. Therefore, the adsorption process of NH_4^+ was dominated by chemical adsorption.

3.2.3 Isotherm adsorption fitting

At different concentrations, the hydrochar influences Cu (II). It is different from the equilibrium adsorption capacity of NH_4^+. The Langmuir isotherm adsorption and the Freundlich adsorption isotherm were fitted to the isotherm adsorption data measured in the experiment. The fitting results are shown in Figure 4.

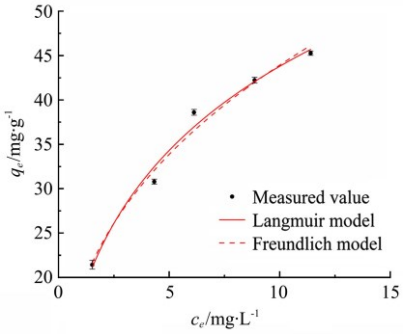

a. Cu (II)

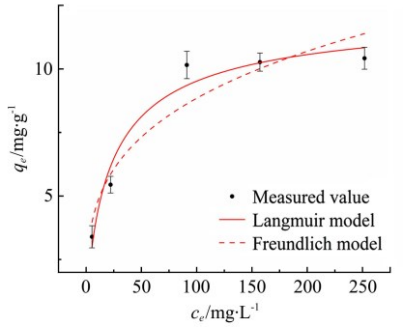

b. NH_4^+

Note: q_e is the adsorption capacity of the adsorbent to the adsorbate per unit mass at the adsorption equilibrium, mg/g; C_e is the equilibrium concentration, mg/L.

Figure 4 Langmuir adsorption isotherm fitting and Freundlich isotherm fitting of Cu (II) and NH_4^+ by hydrochar

The adsorption of Cu (II) by hydrochar had a fitting degree of 0.9771 for the Langmuir isothermal adsorption model. The Freundlich adsorption isotherm model was 0.9543, indicating that the Langmuir isotherm adsorption model was more suitable for describing the adsorption of Cu (II) by hydrochar. According to the adsorption law, the adsorption of Cu (II) on the surface of hydrochar was more inclined to monolayer adsorption[17,24]. Due to the presence of a large number of oxygen-containing functional groups on the surface of the hydrochar prepared by the hydrocharization method, it can chelate with Cu (II) and form a relatively stable chelate compound, so the adsorption of Cu (II) is relatively high. It was also more stable. In addition, some oxygen-containing functional groups on the surface of hydrochar can also form ion exchange adsorption with Cu (II), which is not as good as chelation adsorption. Therefore, the adsorption of Cu (II) by hydrochar was mainly based on chelation, combined with ion exchange to realize the adsorption of heavy metal Cu (II)[18].

The fitting degree of the adsorption of the hydrochar pair was 0.9971 for the Langmuir isotherm adsorption model, and 0.9555 for the Freundlich adsorption isotherm model, indicating that the adsorption of NH_4^+ on the surface of the hydrochar was more inclined to the monolayer adsorption, so the adsorption of NH_4^+ on the surface of the hydrochar was mainly determined by the spatial pore structure of the hydrochar and the development and abundance of surface-active groups. Combined with the results of adsorption kinetics, the adsorption of NH_4^+ by hydrochar has both physical adsorption and chemical adsorption. Among them, ion exchange mainly affected chemical adsorption and worked together with physical adsorption to adsorb NH_4^+.

3.3 Competitive adsorption characteristics of Cu (II) and NH_4^+ in sewage

3.3.1 Effects of pH and ionic strength on Cu (II) adsorption

From Figure 5, the adsorption isotherm curves of Cu (II) were well fitted, and the R^2 was above 0.97. As listed in Table 3, the parameters obtained by fitting the adsorption isotherm curve at a constant pH decrease with the increase in ionic strength. It indicated that the more significant the ionic strength, the lower the adsorption strength of the corresponding ions, and the smaller the adsorption capacity. This may be because the increase of ionic strength makes the concentration of cations in the system compete, and the negative site charges on the surface of the adsorbent are largely occupied, which reduces the electrical adsorption of Cu (II)[5,25]. When the ionic strength was constant, the greater the pH was, the greater the adsorption capacity, and the stronger the adsorption capacity was. This may be because the increase in pH causes the release of protons on the surface of biochar, and the hydroxyl-free ions generated by the hydrolysis of Cu (II) are more readily adsorbed on the surface of biochar, thereby increasing the adsorption capacity[26].

3.3.2 Effects of pH and ionic strength on NH_4^+ adsorption

The adsorption isotherm of NH_4^+ had a good fitness, with R^2 above 0.93, but the Langmuir model had a better fit than the Freundlich model. In Table 4, when the pH is constant, the parameters obtained by fitting the adsorption isotherm curve decreased with the increase of the ionic strength. That indicated the greater the ionic strength, the lower the adsorption strength of the corresponding ions, and the smaller the adsorption capacity. When the ionic strength was constant, the larger the pH was, the stronger the adsorption capacity was. This was because the increase in pH made the content of OH^- increased, and NH_3 is generated and discharged from the system[26].

In comparison, the q_0 value of NH_4^+ was generally lower than that of Cu (II), which indicates that the saturated adsorption amount of Cu (II) in the system was greater than that of NH_4^+, and the total amount of Cu (II) adsorption was also larger. Therefore, Cu (II)

was more competitive for adsorption than NH_4^+. When monovalent and divalent cations coexisted in the system, hydrochar will preferentially adsorb high-valent ions[15]. When Cu (II) was present, a large amount of Cu (II) existed in the form of hydrated ions, occupying the main site, so NH_4^+ does not have an advantage in the competition.

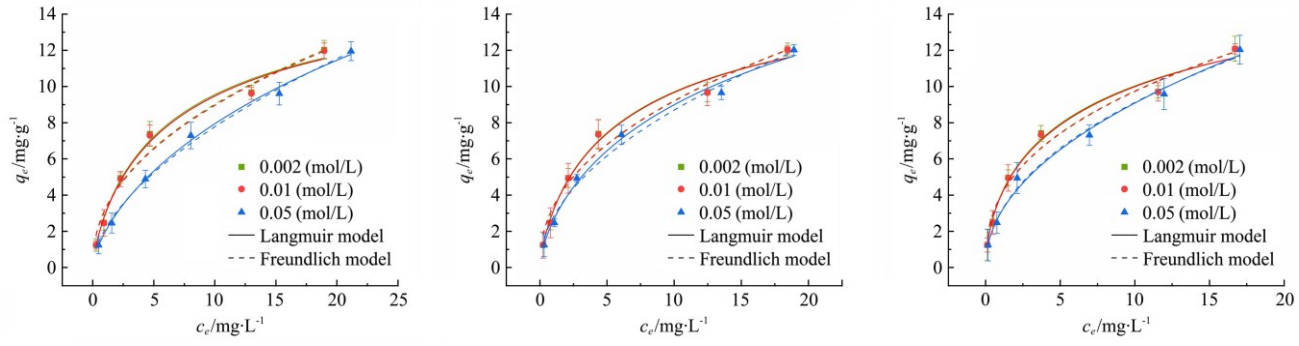

a. pH=4.5 b. pH=5.0 c. pH=5.5

Figure 5 Adsorption isotherm fitting of Cu (II) at different pH and ionic strength

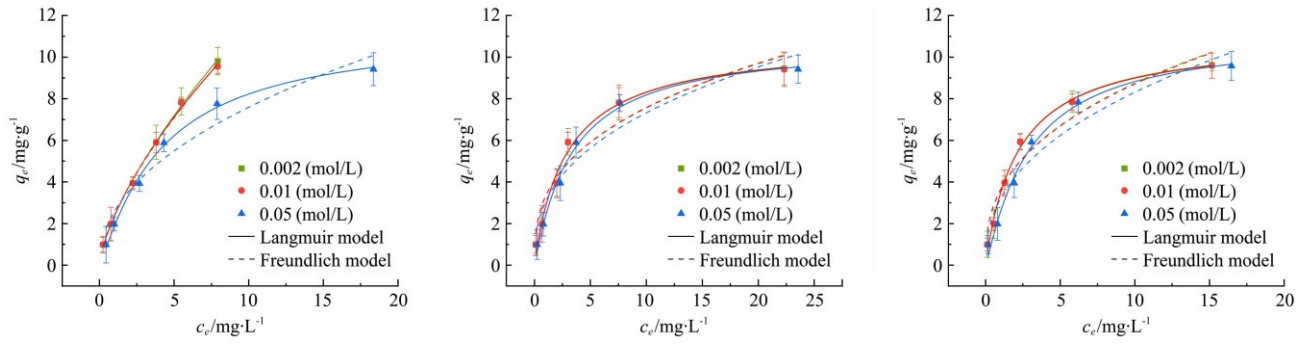

a. pH=4.5 b. pH=5.0 c. pH=5.5

Figure 6 Adsorption isotherm fitting of NH_4^+ at different pH and ionic strength

Table 3 Adsorption isotherm fitting parameters of Cu (II) under different pH and ionic strength conditions

pH	Ionic strength /mol·L^{-1}	Langmuir			Freundlich		
		q_0	b	R^2	K	n	R^2
4.5	0.002	13.763	0.257	0.982	2.709	1.863	0.977
	0.010	15.567	0.124	0.982	1.943	1.658	0.979
	0.050	16.915	0.095	0.996	1.644	1.511	0.993
5.0	0.002	13.543	0.292	0.989	2.884	1.921	0.978
	0.010	14.249	0.205	0.993	2.464	1.801	0.989
	0.050	14.758	0.173	0.993	2.258	1.714	0.989
5.5	0.002	12.763	0.471	0.988	3.559	2.199	0.982
	0.010	13.268	0.298	0.992	3.023	2.074	0.992
	0.050	12.898	0.196	0.973	2.664	1.997	0.972

Table 4 Adsorption isotherm fitting parameters of NH_4^+ under different pH and ionic strength conditions

pH	Ionic strength /mol·L^{-1}	Langmuir			Freundlich		
		q_0	b	R^2	K	n	R^2
4.5	0.002	14.870	0.205	0.998	2.454	1.512	0.998
	0.010	12.303	0.197	0.997	1.937	1.589	0.948
	0.050	11.947	0.169	0.998	1.706	1.590	0.931
5.0	0.002	10.407	0.418	0.987	2.759	2.158	0.961
	0.010	10.679	0.319	0.992	2.360	1.919	0.956
	0.050	11.169	0.239	0.997	2.044	1.752	0.975
5.5	0.002	10.806	0.507	0.994	3.076	2.008	0.945
	0.010	11.250	0.348	0.991	2.653	1.893	0.984
	0.050	11.353	0.311	0.991	2.449	1.792	0.967

Note: q_0 is the saturated adsorption capacity of the adsorbent, mg/g; b is the Langmuir adsorption constant, L/mg; K is the Freundlich adsorption equilibrium constant, reflecting the strength of the adsorption capacity; n reflecting the difficulty of adsorption.

4 Conclusions

1) The carbon content of the modified hydrochar was significantly increased, indicating that the modifier had a specific promoting effect on the hydrothermal reaction; its H/C and O/C atomic ratios decrease, indicating that the modified hydrochar is aromatic and hydrophobic sexual enhancement. The surface morphology of the modified hydrochar was sparser, the carbon microspheres have better sphericity, and the surface functional groups are more abundant than those before the modification, which is conducive to the adsorption of pollutants. The specific surface area and total pore volume of the modified hydrochar increased by 1.65% and 1.32%, respectively, which was conducive to the entry of pollutants into the hydrochar and improved its adsorption efficiency.

2) The dosage and adsorption time of hydrochar influenced the adsorption process of Cu (II) and NH_4^+ in sewage. The adsorption capacity of hydrochar per unit mass decreased gradually with the dosage increase. In the initial stage of adsorption, the adsorption of Cu (II) and NH_4^+ by hydrochar can proceed rapidly, and with the extension of adsorption time, the adsorption rate gradually decreases, and finally reaches equilibrium.

3) The adsorption of Cu (II) and NH_4^+ in sewage by hydrochar was mainly chemical adsorption, mainly affected by chelation and ion exchange. Furthermore, the adsorption was more inclined to monolayer adsorption. Therefore, the adsorption effect was mainly determined by the spatial pore structure on the surface of the hydrochar and the development and abundance of surface-active groups.

4) There was competition in the adsorption of Cu (II) and NH_4^+ in sewage, and the initial pH value and ionic strength will affect

their adsorption. For Cu (II) and NH_4^+, the larger the pH, the stronger the adsorption capacity of hydrochar.

Acknowledgements

This work was financially supported by the State Grid Corporation Science and Technology Project (Grant No. 5400-202031205A-0-0-00), Research and application of rural comprehensive energy recycling technology based on biomass-power-heat coupling and National Dairy Industry and Technology System (CARS-36).

[References]

[1] Font-Palma C. Characterisation, kinetics and modelling of gasification of poultry manure and litter: An overview. Energy Conversion and Management, 2012; 53(1): 92–98.

[2] Zhang S Y, Hong R Y, Cao J P, Takarada T. Influence of manure types and pyrolysis conditions on the oxidation behavior of manure char. Bioresource Technology, 2009; 100(18): 4278–4283.

[3] Kong F K, Shao L, Yang S J, Luo X, Wang W, Ju X X, et al. Application of solid-liquid separation technology in manure water treatment and resource utilization of livestock and poultry breeding. Swine Industry Science, 2017; 34(4): 96–98. (in Chinese)

[4] Yang P Y. The performance of membrane bioreactor treating wastewater from dairy farm. Master dissertation. Beijing: Chinese Academy of Agricultural Sciences, 2019; 75p. (in Chinese)

[5] Herath A, Reid C, Perez F, Pittman Jr C U, Mlsna T E. Biochar-supported polyaniline hybrid for aqueous chromium and nitrate adsorption. Journal of Environmental Management, 2021, 296: 113186. doi: 10.1016/j.jenvman.2021.113186.

[6] Liu Q. Preparation of coconut shell-sludge composite activated carbon and its study on the adsorption of Cr(VI) in simulated wastewater. Master dissertation. Chengdu: Southwest Petroleum University, 2018; 69p. (in Chinese)

[7] Niinipuu M, Latham K G, Boily J-F, Bergknut M, Jansson S. The impact of hydrocharization on the surface functionalities of wet waste materials for water treatment applications. Environmental Science and Pollution Research, 2020; 27(19): 24369–24379.

[8] Kaewtrakulchai N, Putta A, Pasee W, Fuangnawakij K, Panomsuwan G, Eiad-ua A. Magnetic carbon nanofibers from horse manure via hydrocharization for methylene blue adsorption. IOP Conference Series: Materials Science and Engineering, 2019; 540(1): 12006. doi: 10.1088/1757-899X/540/1/012006.

[9] Ma Q Y, Logan T J, Traina S J. Lead immobilization from aqueous-solutions and contaminated soils using phosphate rocks. Environmental Science & Technology, 1995; 29(4): 1118–1126.

[10] Wu H Y. Adsorption behavior of Pb(II) and phenol by activated carbon prepared by shaddock peel. Master dissertation. Taiyuan: Taiyuan University of Science and Technology, 2020; 72p. (in Chinese)

[11] Zhou S M, Han L J, Yang Z L, Ma Q L. Influence of hydrocharization temperature on combustion characteristics of livestock and poultry manures. Transactions of the CSAE, 2017; 33(23): 233–240. (in Chinese)

[12] Yuan J. Preparation of sewage sludge hydrothermal charcoal and its removal effect on heavy metals in water. Master dissertation. Shanghai: Donghua University, 2019; 100p. (in Chinese)

[13] Yu J G. Hydrothermal modification of agricultural waste biomass charcoal and study of its adsorption performance. Master dissertation. Dalian: Dalian University of Technology, 2018; 71p. (in Chinese)

[14] Qiao N. Hydrocharization of corncob and pinenut shell and the adsorption performance of its product. Master dissertation. Dalian: Dalian University of Technology, 2015; 65p. (in Chinese)

[15] Sun Y Y. Co-transport simulation and model parameter analysis of heavy metals and ammonium nitrogen in the soil. Master dissertation. Qingdao: Qingdao University, 2013; 94p. (in Chinese)

[16] N.Wibowo, L.Setyadhi, D.Wibowo, J.Setiawan, S.Ismadji. Adsorption of benzene and toluene from aqueous solutions onto activated carbon and its acid and heat-treated forms: Influence of surface chemistry on adsorption. Journal of Hazardous Materials, 2007; 146(1-2): 237–242.

[17] Martins A C, Pezoti O, Cazetta A L, Bedin K C, Yamazaki D A S, Bandoch G F G, et al. Removal of tetracycline by naoh-activated carbon produced from macadamia nut shells: Kinetic and equilibrium studies. Chemical Engineering Journal, 2015; 260: 291–299.

[18] Zhang P Z, Zhang X X, Yuan X R, Xie R Y, Han L J. Characteristics, adsorption behaviors, Cu(II) adsorption mechanisms by cow manure biochar derived at various pyrolysis temperatures. Bioresource Technology, 2021; 331: 125013. doi: 10.1016/j.biortech.2021.125013.

[19] Chang M Y, Juang R S. Adsorption of tannic acid, humic acid, and dyes from water using the composite of chitosan and activated clay. Journal of Colloid and Interface Science, 2004, 278(1): 18–25.

[20] Cai J. The study of adsorption of cadmium in aqueous solution by phosphate-modified bamboo biochar. Master dissertation. Wuhan: Huazhong University of Science and Technology, 2018; 72p. (in Chinese)

[21] Han L J, Li Y L, Liu X, Han Y H. Review of biochar as adsorbent for aqueous heavy metal removal. Transactions of the CSAM, 2017; 48(11): 1–11. (in Chinese)

[22] Li H, Xiao D L, He H, Lin R, Zuo P L. Adsorption behavior and adsorption mechanism of Cu(II) ions on amino-functionalized magnetic nanoparticles. Transactions of Nonferrous Metals Society of China, 2013; 23(9): 2657–2665.

[23] Iida T, Amano Y, Machida M, Imazeki F. Effect of surface property of activated carbon on adsorption of nitrate ion. Chemical & Pharmaceutical Bulletin, 2013; 61(11): 1173–1177.

[24] Jin K, Lu Q, Ma L J, Li H J, Shi Z J. Preparation of walnut shell carbon and its adsorption of ammonia-nitrogen wastewater. Biomass Chemical Engineering, 2021; 55(1): 63–69. (in Chinese)

[25] Rajabi H, Mosleh H M, Prakoso T, Ghaemi N, Mandal P, Lea-Langton A, et al. Competitive adsorption of multicomponent volatile organic compounds on biochar. Chemosphere, 2021; 283: 131288. doi: 10.1016/j.chemosphere.2021.131288.

[26] Karami H. Heavy metal removal from water by magnetite nanorods. Chemical Engineering Journal, 2013; 219: 209–216.